Curr Radiol Rep (2017) 5:31
DOI 10.1007/s40134-017-0227-7

DUAL ENERGY CT (S NICOLAOU AND M MOHAMMED, SECTION EDITORS)

Gastrointestinal Imaging: Emerging Role of Dual-Energy Computed Tomography

Ismail Tawakol Ali[1] · Cyrus Thomas[2] · Khaled Y. Elbanna[1] · Mohammed F. Mohammed[1] · Ferco H. Berger[3] · Faisal Khosa[1]

Published online: 23 May 2017

Abstract
Purpose of Review The clinical and research applications of dual-energy computed tomography (DECT) are evolving and exponentially growing. In this article, we focus on the different applications of DECT for gastrointestinal (GI) imaging. The basic principles of DECT are important to understand its ability to differentiate tissues via application of two energy spectra.
Recent Findings Different DECT techniques and scanners currently used are discussed to highlight their advantages and limitations for generating dual-energy datasets. The advantage of generating virtual non-contrast, virtual monoenergetic, and iodine overlay images will be described for evaluation of bowel pathology, including inflammatory, vascular, and neoplastic conditions, as well as in the setting of acute trauma.
Summary This review focuses on the applications of DECT across wide range of GI pathologies throughout the large and small bowel. With continuous research and further development of this technology, the use of DECT in imaging and evaluating the bowel holds a promising future.

This article is part of the Topical collection on *Dual-Energy CT*.

✉ Faisal Khosa
fkhosa@hotmail.com

Ismail Tawakol Ali
ismailtawakol@gmail.com

[1] Division of Emergency & Trauma Radiology, Department of Radiology, Vancouver General Hospital, 899 12th Avenue W, Vancouver, BC V5Z 1M9, Canada

[2] Faculty of Medicine, University of British Columbia, Vancouver, BC, Canada

[3] Department of Radiology, Sunnybrook Health Sciences Centre, University of Toronto, Toronto, ON, Canada

Keywords Dual-energy CT · Bowel imaging · Bowel ischemia · GI bleeding · Colon cancer · Bowel trauma

Introduction

Computed tomography (CT) plays an important role in the evaluation of the abdomen and pelvis due to its universal availability, high temporal and spatial resolution, and scanning speed [1•]. CT conventionally utilizes a single, polychromatic X-ray beam, which is defined by the highest potential for photons in its spectrum, e.g., a 120 kVp (peak kilovolt) beam would be one in which the X-ray beam spectrum has the highest potential of 120 keV (kiloelectronvolt). Dual-energy CT (DECT) is an evolving technology, which adds value to CT imaging, where the same volume is imaged by two differing energy spectra [2]. The purpose of this article is to review the basic principles, technical approaches, and the applications of DECT in small and large bowel pathology including inflammatory conditions, primary and metastatic neoplasms, vascular abnormalities, trauma, and appendicitis.

Technical Developments

Basic Principles of Dual-Energy CT

CT makes use of the fact that different tissues in the human body interact in different ways with the photons in the X-rays transmitted through the body. Interaction of bodily tissues with photons results in Compton scatter and photoelectric effect [1•, 2, 3]. Compton scattering occurs when the incident X-ray photon ejects a weakly bound outer shell electron [4]. Alternatively, photoelectric absorption occurs

when the incident x-ray photon interacts with a tightly bound inner (K-shell) electron. The photon is then completely absorbed, consequently ejecting the K-shell electron without resulting scattered radiation [4]. Photoelectric interactions are dependent on the binding energy of the K-shell electron, which is proportionate to the atomic number (see Table 1) [4–6]. The likelihood of photoelectric absorption increases as the energy of the incident photon approaches the K-shell binding energy [5]. The "K-edge" refers to the sharp rise in attenuation that is seen at energy levels just above the K-shell binding energy because photons with a greater energy than the K-shell threshold are more likely to be absorbed [1•]. Conventional CT uses a polychromatic X-ray beam, which is defined by the highest potential for photons in its spectrum, e.g., a 120 kVp (peak kilovolt) beam would be one in which the X-ray beam spectrum has the highest potential of 120 keV (kiloelectronvolt). This single spectrum is used to characterize the attenuation of body tissues to a certain degree. Attenuation of any given tissue is different for different X-ray spectra, however, for each tissue, there is a defined relationship of attenuation behavior between the spectra. DECT uses two X-ray spectra to generate its datasets instead of the one X-ray spectrum of conventional CT. Given the tissue-dependent relationship of attenuation in the two X-ray spectra, DECT allows the differentiation of materials such as calcium and iodine from soft tissues due to their differences in K-edges and attenuation at different energy levels [1•, 7].

Different Techniques of DECT

Consecutive Acquisition DECT

Two consecutive scans are performed, each with a specific X-ray spectrum. This approach acquires two scans at fixed energy spectra, for example, 140 and 80 kVp at the same anatomic level [1•]. The advantage of this technique is the full field of view and application of dose modulation in both acquisitions. The main limitations with this technique include the delay between the two separate acquisitions, for example, at 80 and at 140-kVp, and asynchronous nature of data acquisition [1•]. A more recently developed approach to consecutive acquisition—also known as *Slow kV Switching*—DECT uses two consecutive helical scans taken at 80 and 140-kVp using a single-source CT system [7]. The use of a non-rigid three-dimensional image registration process that registers each respective energy dataset can correct for motion between the two acquisitions [8].

Table 1 K-edges of common elements: the figure from Nogueira et al. outlines the K-edges and atomic numbers of elements common seen on CT scans

Substance	K-Edge (keV)	Atomic number (*Z*)
Hydrogen	0.01	1
Carbon	0.28	6
Nitrogen	0.40	7
Calcium	4.00	20
Iodine	33.20	53
Barium	37.45	56

The K-edges of Hydrogen, Carbon, and Nitrogen are too low and similar to each other to be differentiated using DECT. Calcium, Iodine, and Barium, however, have K-edges that are appreciably different from each other and importantly, these substances can be well differentiated from soft tissues during dual-energy imaging [7]

Dual-Source DECT

Dual-source CT scanners use two X-ray tube-detector pairs mounted nearly perpendicularly [1•]. Operating the two X-ray tubes at different X-ray spectra allows for acquisition with minimal time delay at any given anatomical location, resulting in close spatial registration [9]. A better separation of the applied spectra results in a more robust characterization of the different materials, improving dual-energy interrogation [10]. A tin filter may be used at the high-energy spectrum in some dual-source CT systems to filter out the lower-energy photons, further improving the spectral separation of the DECT acquisition. A limitation of this technique is that the near perpendicular setup of the two X-ray sources and detectors predisposes to cross-scatter radiation [1•, 9].

Fast Voltage Switching DECT

This technique utilizes high-frequency, low-capacitance generators. The single X-ray tube that switches voltages during gantry rotation allows for faster data sampling [11, 12]. There is virtually no time delay between the acquisitions of the two different X-ray spectra for any given anatomy, which could limit motion effects during scanning [11].

The fast switching time between low- and high-energy acquisitions results in rise and fall effects during the integration period thus, decreasing the spectral separation for a given dataset [13]. Pseudostratified bowel wall artifact has been reported with the use of rapid kV switching technique. It refers to pseudopneumatosis, pseudohyperenhancement, or pseudohypoenhancement and is commonly seen in the jejunal segments on iodine density imaging [14].

Layer Detector DECT

Layer detector DECT uses a double-layer detector technology where the top layer contains zinc selenide (ZeSn) or

cesium iodide (CsI) and the bottom contains gadolinium oxysulfide (Gd_2O_2S). This setup allows the collection of dual-energy data via a single X-ray source CT acquisition [15, 16]. The superficial layer absorbs low-energy photons while the deeper one absorbs high-energy photons [16].

Limitations of layer detector DECT include poor soft tissue contrast due to predominance of high-energy and low-contrast projections over low-energy and high-contrast projections and high radiation exposure [1•, 15, 16].

Dual-Energy CT Imaging Reconstruction Methods

Non-material-Specific Display

Non-material-specific display combines the data from low- and high-energy images into a single dataset [1•]. It has the advantage of exploiting the entire radiation dose spectrum delivered during a DECT acquisition, which effectively reduces noise [17]. These images are obtained using a "linear blending ratio" where a user-selected ratio between the high- and low-energy acquisitions can reproduce the image quality of a single-energy acquisition and can be adjusted depending on the low/high-energy spectrum combinations used to acquire the scan [17–19]. To maximize the contribution from high-contrast/low-energy datasets, new functions including binary blending, slope blending, Gaussian-modified sigmoid, and piecewise functions have been developed [20]. A limitation of this method is that this display may present inaccuracies in absolute CT numbers for attenuation measurements [1•].

Material-Specific Display

In material-specific display, substances are differentiated based on their unique absorption of X-rays at different energy levels due to the differences in their atomic number. This enables labeling of materials and decomposition of the images. The most commonly differentiated materials are iodine, calcium, fat, and soft tissue [1•]. If chosen, intravenously administered contrast containing iodine can be differentiated from soft tissue and fat, generating iodine distribution maps or virtual non-contrast-enhanced (VNC) images by subtracting it from the images. Evidence suggests that VNC image quality is comparable to that of a conventional non-enhanced acquisition; therefore VNC images may obviate the need for true non-contrast phase [21].

Energy-Specific Display

DECT allows the reconstruction of virtual monochromatic images (VMIs) which are synthesized in either a projection or image space domain. These images have relevant clinical applications, including beam-hardening correction, optimization of image quality, and metal artifact reduction [1•].

VMI could also be used to improve contrast-to-noise ratio (CNR). Early evidence has shown that optimum iodine CNR is achieved within the 60–70 keV range and is associated with the lowest amount of noise in VMI reconstructions [19]; however, the bowel specifically has been shown to be better assessed at the 40–50 keV range despite the increase in background noise [22, 23]. Optimized VMI may also improve image quality compared to that of a conventional 120 kVp CT with a similar radiation dose [19].

Dual-Energy ct in Imaging Gastrointestinal Pathology

Special Contrasts Used in DECT

Positive enteric contrast material is of diagnostic value in cases of suspected bowel leak and obstruction; however, it suffers the disadvantage of obscuring the bowel wall enhancement. On the other hand, neutral enteric contrast facilitates the detection of abnormal bowel wall enhancement but has a limited value in detection of bowel leak [24]. A third type of contrast material has been investigated in vivo as an enteric contrast that can be digitally subtracted from intravenous iodinated contrast material [25, 26].

At 80:140 kVP, the attenuation ratios of Bismuth, Tantalum, and Tungsten are 1.3, 1.0, and 1.0, respectively, compared to 1.7 for iodine. The significant difference in attenuation ratios of both Tantalum and Tungsten (1.0) relative to iodine (1.7) allows satisfactory digital subtraction of enteric tantalum and tungsten from iodinated bowel wall in double-contrast DECT resulting in a significant improvement of bowel wall assessment on iodine density map of double-contrast DECT compared to double-contrast conventional CT. In addition, these materials have a high atomic number (Z) leading to an increase in attenuation on 70-keV VMIs that add to its value as a positive enteric contrast [26].

Inflammatory Conditions

Inflammatory bowel disease (IBD) broadly defines acute or chronic presentation affecting the GI tract; the two main intestinal disorders being ulcerative colitis (UC) and Crohn's disease (CD). In UC, the inflammation is limited to the large intestine and affects only the intestinal mucosa. With CD however, inflammation may occur at any part along the GI tract and is usually transmural in nature [27].

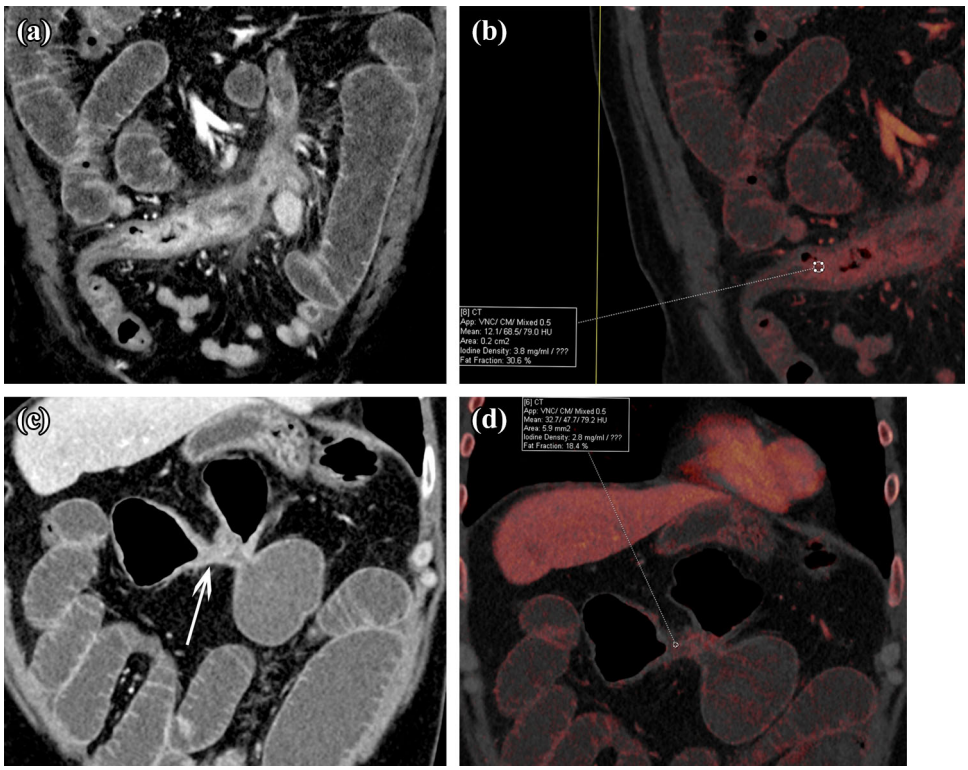

Fig. 1 A 28-year-old male with Crohn's disease complaining of worsening abdominal pain. **a** Coronal VMI, **b** coronal IOI: demonstrate the increased mural enhancement with corresponding increased iodine density in active inflammatory stricture with enterocolic fistula. **c** Coronal VMI, **d** coronal IOI: demonstrate less contrast enhancement and decreased iodine density in chronic fibrotic stricture of the transverse colon/splenic flexure and pseudosacculation

CT imaging for inflammatory conditions can distinguish the location and length of the inflamed segments, the extent of bowel wall thickening, and the involvement of nearby soft tissues [28•]. On CT enterography, the most sensitive indicator of active Crohn's disease is mural hyperenhancement [29].

Studies evaluating the role of DECT in IBD have noted unique advantages including its usefulness at highlighting alterations in bowel wall enhancement patterns via iodine imaging [28•]. Furthermore, iodine overlay images (IOIs) serve as a marker of tissue contrast uptake and may be more sensitive to subtle areas of bowel wall hyperenhancement compared to conventional CT images [30]. In our experience, the active skip lesions of Crohn's disease can stand out against the spared bowel segments by using low-keV VMIs that demonstrate the segments of mural hyperenhancement with corresponding high iodine uptake on IOIs. The degree of enhancement may be helpful to differentiate between disease activity and focal stricture with predominant fibrosis (Fig. 1).

In cases of acute appendicitis, CT has a diagnostic accuracy rate of 93–98% [31]. Appendiceal diameter of 6–10 mm may be considered indeterminate as a single parameter for diagnosis and should be interpreted along with additional signs including appendiceal wall thickening, appendiceal wall hyperenhancement, appendicolith, and periappendiceal fat stranding [32]. In cases of early appendicitis, IOIs may be able to detect subtle wall hyperenhancement even in the absence of periappendiceal fat stranding [28•].

In our experience, these signs can be better illustrated on DECT. Low-keV VMI facilitates detection of subtle mural hyperenhancement of the appendix, and periappendiceal fat stranding can be identified on IOIs. In some cases, it may be difficult to differentiate oral contrast from a calcified appendicolith at the base of the appendix, however; by assessing VNC images, oral contrast can be subtracted while an appendicolith would remain. The same principle can be applied for differentiation of a subtle mural soft tissue nodule from appendicolith by confirming iodine uptake on iodine overlay images. In addition, VMIs may also detect areas of early gangrene in the appendiceal wall, which may help identify patients that may be at higher risk for perforation.

Primary epiploic appendagitis results from torsion of epiploic appendages, leading to ischemic infarction and commonly appears as oval fat-density lesion abutting the colonic wall surrounded by inflammatory changes [33]. From our observations, there is little to no iodine uptake by the hyperattenuating rim or the inner fat density, representing an infarcted appendage, on IOIs, compared to mild increase in iodine uptake in the surrounding inflamed fat (Fig. 2).

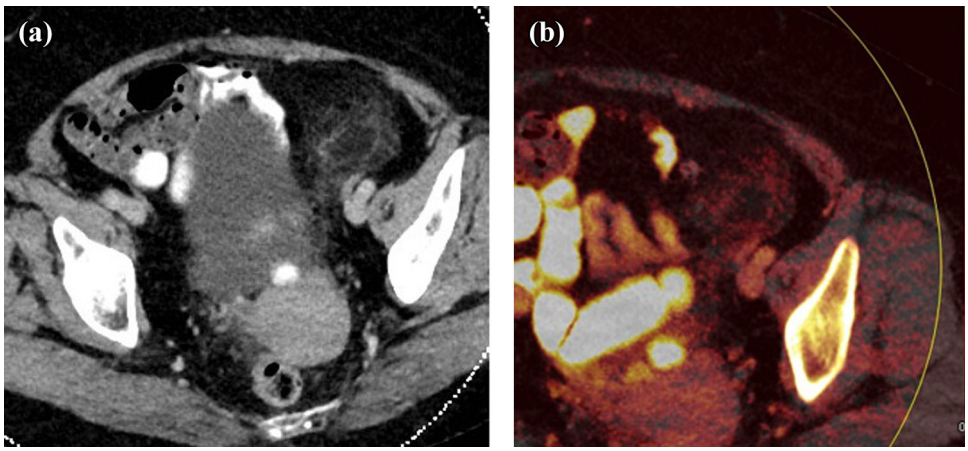

Fig. 2 A 59-year-old female with left lower quadrant pain (**a**) contrast-enhanced Axial CT images demonstrate the classic appearance of epiploic appendagitis as a fat-density lesion with a thin rim and surrounding fat stranding, (**b**) axial IOI demonstrates higher iodine uptake of the surrounding fat secondary to inflammation and lack of iodine uptake within the infarcted epiploic appendage

Evaluation of Bowel Neoplasms

Small Bowel

Primary cancer of the small intestine is quite uncommon. For small bowel adenocarcinoma, the duodenum is the most frequently involved segment while the ileum is the commonest site for small bowel neuroendocrine tumor, and lymphoma [34].

In cases of neuroendocrine tumor of the small bowel, it is often difficult to identify the primary tumor on CT due to its small size. It appears as a hypervascular polypoid or plaque-like mural lesion which is generally <2 cm in size [35]. In our experience, low-energy VMI especially at (40 keV) and IOI improve detection of hypervascular mural nodules such as neuroendocrine tumors, which contributes to detection and localization of these tumors (Fig. 3).

In a study by Shinya et al., Gastrointestinal stromal tumor (GIST) and neuroendocrine tumors (NET) have mean attenuation values significantly higher than those of adenocarcinoma and lymphoma in the arterial and enteric phases. Mean attenuation of GIST was 121.79 HU and for NET was 123.95 HU at 120 kVp polychromatic conventional CT [36•]. Future investigation may be directed to assess the validity of considering iodine density as a differentiating point between the different types of small bowel tumors.

A recent study by Martin et al. demonstrates that the signal-to-noise ratio (SNR) and contrast-to-noise ratio (CNR) at 40-keV VMI reconstructions of DECT are significantly higher than linearly blended images which simulate routine single-energy 120-kV acquisition, contributing to better diagnostic evaluation of tumors [37] (Fig. 4).

Large Bowel

Colorectal cancer is a common malignant tumor and one of the leading causes of cancer related deaths in North America, the most common type being adenocarcinoma [38]. Imaging with CT Colonography (CTC) is considered a minimally invasive tool to

Fig. 3 An 83-year-old man, with known case of carcinoid tumor of the small bowel (**a**) mixed images (**b**) VMI & (**c**) IOI: with multifocal hyperenhancing mucosal lesion of the small bowel (*arrows*) and mesenteric calcified metastasis (*dotted arrow*): the multifocal mural nodules of the primary tumor are more conspicuous on VMI and IOI compared to the mixed images

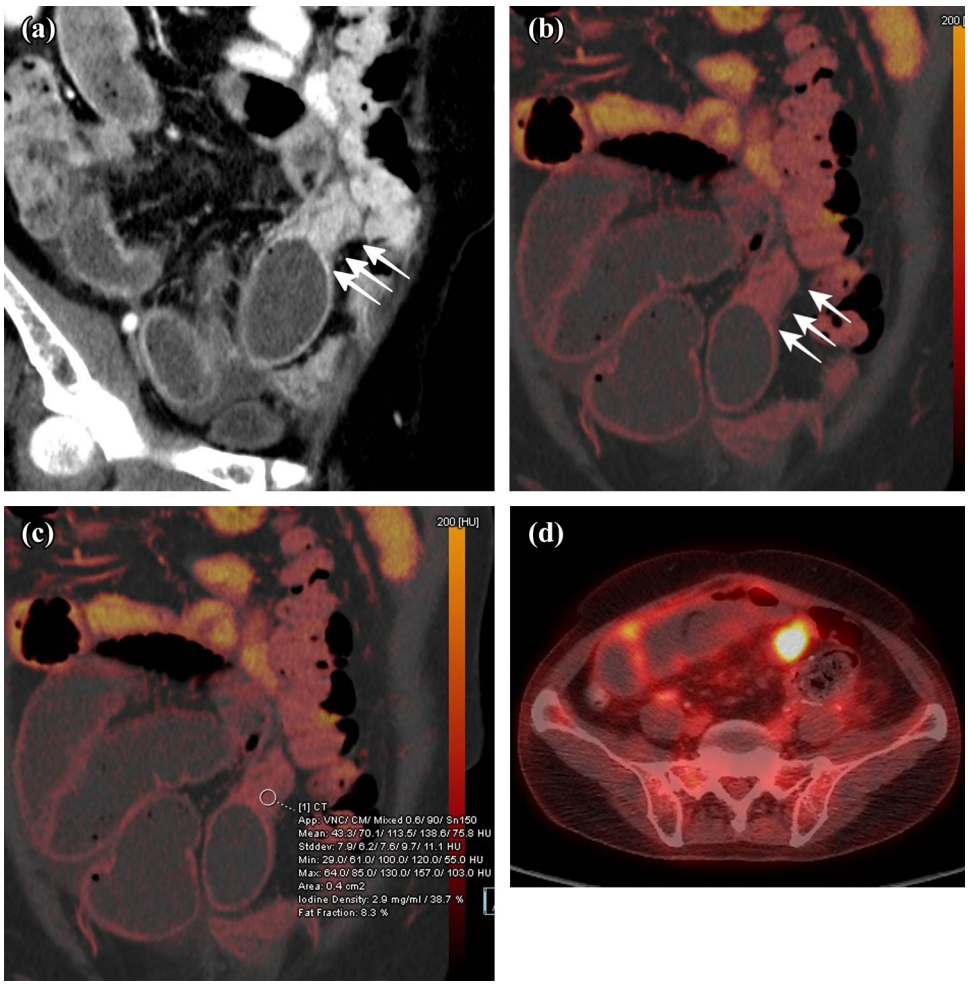

Fig. 4 A 68-year-old male with history of resected sigmoid cancer 4 years ago came into ED with abdominal distension (**a**–**c**) 40-keV VMI and IOI clearly demonstrate a focal stricture of the mid-ileum (*arrows*) with upstream small bowel dilatation, the appearance is suggestive of malignant small bowel obstruction secondary to subserosal recurrent/metastatic disease, **d** 18F-FDG PET/CT scan demonstrates a corresponding FDG avid uptake of the soft tissue mass. Histopathology revealed submucosal mass with mucosal ulceration consistent with recurrent deposit of adenocarcinoma of the colon

colonic evaluation [39]. Preoperative staging of colorectal cancer can be achieved by contrast-enhanced CTC as an alternative to Optical Colonoscopy, due to the accurate detection and localization of the tumor with CTC [40, 41].

DECTC can be performed on the day of colonoscopy to avoid repeated bowel cleansing. In patients with colon cancer, a colonic polyp or mass can be differentiated from other filling defects by the presence of contrast enhancement. Therefore, an additional prone position in CTC may not be required to differentiate between these two entities. Furthermore, colonic adenomas and carcinomas can be reliably discriminated from lipomas that have no significant enhancement. However, carcinomas cannot be reliably distinguished from adenomas due to similarity in enhancement [42].

On IOIs, the colonic wall is outlined against the colonic lumen and pericolic fat [43]. This allows detection of tumor as a focal wall thickening with increased iodine density and assesses tumor spread beyond the muscularis propria [11, 44]. According to a recent study by Schaeffer et al., evaluation of local tumor invasion (T1/T2 vs. T3/T4) can be accurately performed with DECTC [42] (Fig. 5).

Quantitative iodine density measurement can discriminate between low- and high-grade colorectal carcinomas. In a study by Gong et al. employing high-grade tumors have Iodine density of 26.27 ± 3.10 mg/mL in venous phase compared to iodine density of 21.90 ± 3.11 mg/mL in low-grade tumors [39].

DECT is a promising tool in detection of metastatic locoregional lymphadenopathy in patients with colorectal cancer. In a recent study by Kato et al., the iodine concentrations of metastatic lymph nodes were significantly lower than non-metastatic lymph nodes in both late arterial and portovenous phases, with an iodine concentration of a 2.1 mg/ml serving as a discriminative cut-off value on the portovenous phase [45].

Evaluation of GI bleeding

Gastrointestinal bleeding (GIB) is a common condition associated with significant morbidity and mortality [46].

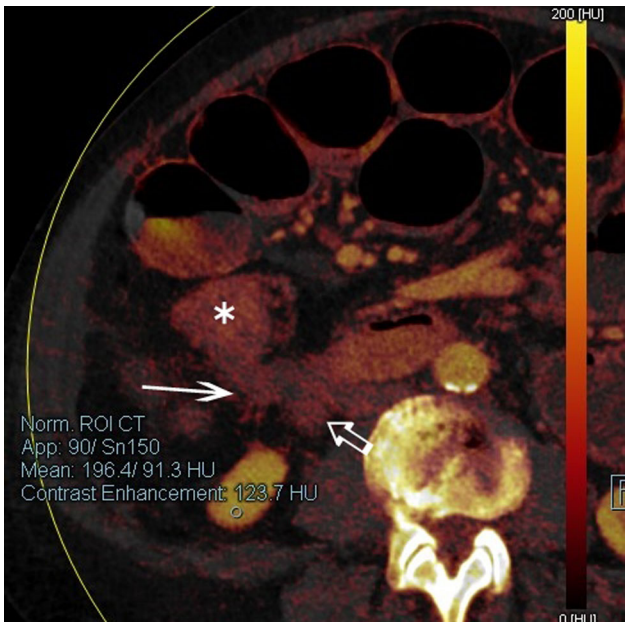

Fig. 5 A 66-year-old male presented with signs of bowel obstruction. Axial CT with IOI clearly demonstrates the extension of the ascending colon adenocarcinoma (*asterisk*) to the pericolic fat, visceral peritoneum (*long arrow*), and invading D2/D3 junction of the duodenum (*short arrow*) that has been confirmed intraoperatively

Bleeding proximal to the ligament of Trietz is defined as upper GIB, while bleeding from the small bowel distal to the ligament of Trietz as well as from the colon and rectum is referred to as lower GIB. Common causes of upper GIB include mucosal erosions, peptic ulcers, tumors, inflammatory, or diverticular conditions, typically present with hematemesis, melena, or coffee ground vomiting. On the other hand, angiectasia/angiodysplasia, neoplasms, inflammatory, or diverticular diseases are common causes of lower GIB, frequently presenting with melena, hematochezia, or rectal bleeding [47, 48]. Upper GI endoscopy, capsule endoscopy, colonoscopy, radionuclide imaging, and catheter angiography are commonly used methods of investigation [46].

CT enterography is indicated in silent obscure lower GIB allowing detection of small vascular lesions as a cause of bleeding. The enhancing bowel wall lesions and active bleeding are detected on a background of neutral enteric contrast material. CT angiography is important for localization of active bleeding in cases of massive bleeding as endoscopic view is limited by excessive blood [47, 48].

The lower-energy spectrum of dual-energy CT provides a contrast resolution within the vessels more than the conventional CT technique, leading to reduction in the required dose of the intravenous (IV) contrast media. Calcium within the bone and calcified plaque can be distinguished from iodinated contrast material. This allows automatic or semi-automatic subtraction of vascular calcification from the enhancing vascular lumen [49, 50].

Similarly, iodine can be subtracted from the enhanced dataset to generate VNC images obviating the need for non-enhanced phase as a part of the traditional triphasic CT protocol performed for cases of GIB. Therefore, the dual-phase CT that includes arterial and a dual-energy portal venous phase has a radiation dose less than that of traditional triphasic CT by 30% [1•, 51].

In cases of acute GIB, IOIs of DECT have been shown to be more accurate than conventional CT due to its ability to demonstrate subtle areas of enhancement and contrast extravasation, as well as quantifying iodine in areas of suspected bleeding [46] (Fig. 6).

Evaluation of Bowel Ischemia

The causes of small bowel ischemia include arterial occlusion (60–70%), venous occlusion (5–10%), strangulated bowel obstruction (10%), and low-flow states (20%) [52]. The role of non-contrast CT is to assess atherosclerotic calcification or bowel intramural hemorrhage, while contrast-enhanced CT enables the detection of vascular filling defects and can estimate ischemia severity [53].

The appearance of the bowel is variable according to the cause and severity of ischemia. Arterial occlusion is associated with abnormally thin bowel wall with decreased enhancement but it could be thickened in reperfusion state. On the other hand, bowel wall thickening with edema or hemorrhage occurs with venous ischemia and strangulation [52]. Other findings include mesenteric fat stranding with free fluid confined to the territory of ischemia, pneumatosis intestinalis, and portomesenteric venous gas [54].

Since the attenuation difference between perfused and non-perfused tissues is accentuated at lower-energy levels, an ischemic bowel segment can be more easily distinguished from non-ischemic bowel on DECT. A recent study by Potretzke et al. signifies that monoenergetic imaging at 51 keV results in a two-fold increase in attenuation difference between perfused and ischemic bowels when compared to conventional imaging at 120 kVp [55•]. IOIs augment the discrimination between ischemic and perfused bowel segments [55•, 56•] (Fig. 7).

In cases of acute small bowel obstruction, conventional polychromatic CT has a limited sensitivity to detect ischemic non-viable segments. The most reliable sign for detecting an ischemic segment is absent or diminished enhancement of the bowel wall which is challenging to identify on conventional polychromatic CT with confidence. Low-energy VMI reconstructions (around 40–70 keV) have almost twice the contrast resolution compared to polychromatic CT. However, owing to increased noise and reduced spatial resolution, low-kV

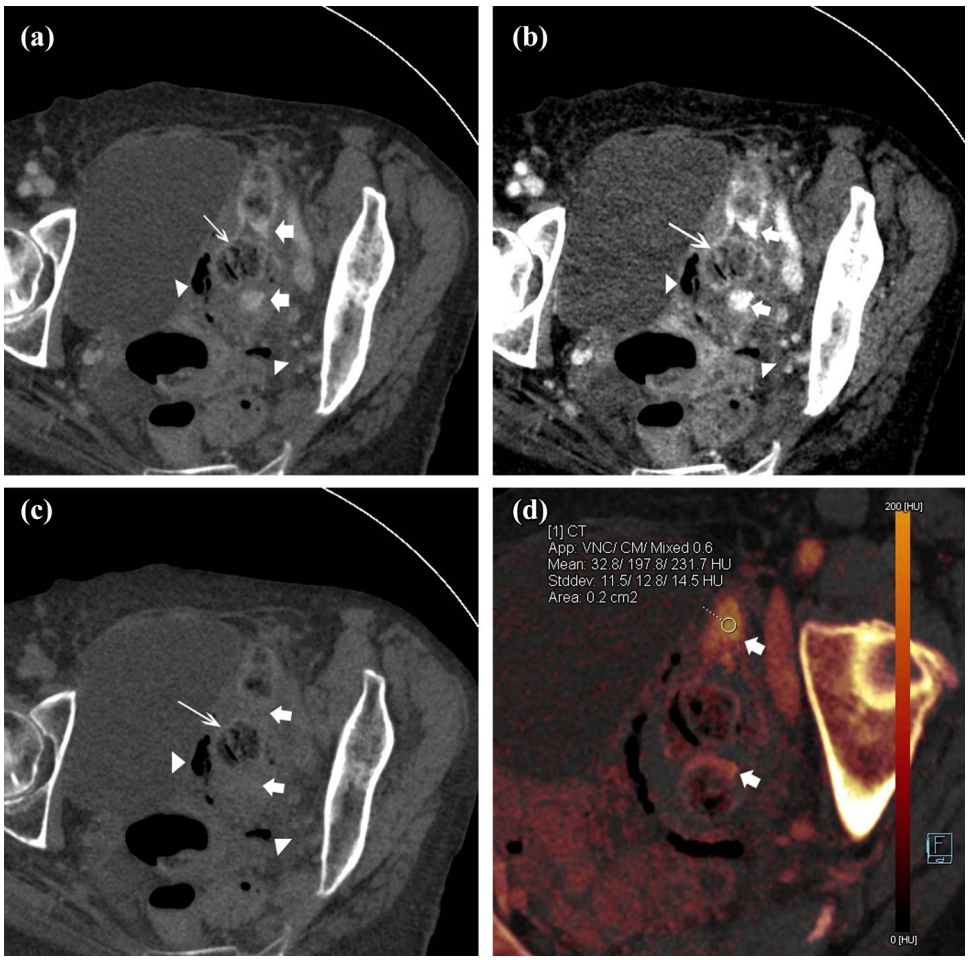

Fig. 6 An 87-year-old female complaining of several days of nausea and vomiting, as well as abdominal pain. Axial CT images after IV contrast only, demonstrating the rectosigmid colon and urinary bladder. **a** Mixed image, **b** 40-keV VMI, **c** 190-keV VMI, **d** IOI. In addition to the extraluminal air (*arrow heads*), there are foci of active bleeding (*thick arrows*) close to the site of perforation images that is difficult to be differentiated from the hyperdense fecal material (*thin arrows*) on mixed CT (**a**) with 40 Kev VMI (**b**) the extravasated vascular contrast has a higher attenuation compared to the fecal material while on 190 keV (**c**) the contrast is subtracted. The appearance is in keeping with active bleeding that was further confirmed by IOI (**d**). Perforated stercoral ulcer with bleeding was found intraoperatively

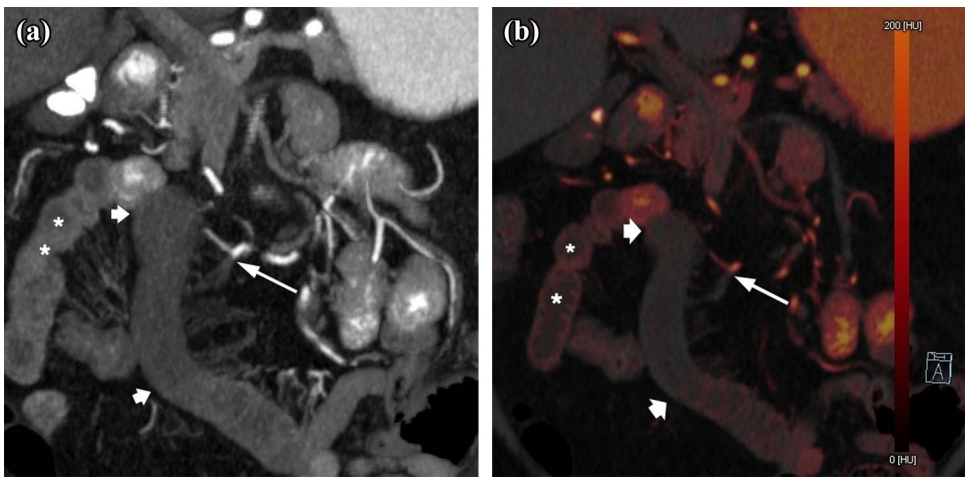

Fig. 7 A 79-year-old male with atrial fibrillation sudden onset epigastric pain and tenderness. **a** Coronal CT VMI; **b** coronal IOI demonstrate cut-off of a jejunal branch of the ileocolic artery (*long arrow*) with corresponding lack of enhancement and decreased iodine uptake of the ischemic bowel segment (between *short arrows*) compared to the normally perfused bowel (*asterisks*)

VMI reconstructions are best used as an additional helpful tool rather than a replacement of conventional imaging [57].

Intramural hemorrhage commonly involves a short segment of small bowel and may even mimic a focal mass, while a longer segment is usually affected in bowel ischemia [58]. DECT with IOIs and VNC images can differentiate intramural hemorrhage from contrast material extravasation with a confidence higher than that of conventional CT [59, 60]. This advantage can be further employed in differentiating intramural hemorrhage of the bowel from mural hyperenhancement that can be seen in

bowel ischemia. In our experience, by subtracting iodine, intramural hemorrhage remains hyperdense on VNC while segmental hyperenhancement has a high iodine density on IOIs and becomes iso- to hypointense on VNC images depending on the degree of edema. In addition, hyperenhancing bowel wall demonstrates higher attenuation values at low-kV VMI reconstructions, while intramural hemorrhage increases in attenuation at high-kV VMI reconstructions (140 keV and greater).

Trauma

Computed tomography (CT) is the main diagnostic study in assessment of the hemodynamically stable patient with penetrating trauma to the abdomen or pelvis [61]. In such cases, CT with both enteric and intravenous contrast materials is used to help in evaluation of bowel injury [62]. It may be difficult in some cases to differentiate enteric contrast leak due to bowel injury from intravenous contrast leak from vascular injury, since they are similarly hyperdense. DECT is unable to differentiate the currently used enteric contrast and intravenous contrast materials as they have similar attenuation ratios. In an experimental animal model study by Mongan et al., DECT demonstrated a higher accuracy and a greater confidence in distinguishing enteric Bismuth subsalicylate from vascular contrast when compared to conventional CT. Newer contrast materials suitable for clinical practice may be used in these challenging cases [63].

In blunt abdominal trauma, CT abdomen has an important role in the detection of significant bowel and mesenteric injuries that require surgical management. CT signs that are specific for significant bowel and mesenteric injuries include bowel wall defects; pneumoperitoneum, pneumoretroperitoneum, and mesenteric free air; enteric contrast leak; vascular contrast extravasation from mesenteric vessels; and diminished or loss of bowel wall enhancement [64]. CT abdomen with arterial and portal venous phases is essential to avoid errors in interpretation of the traumatic findings [65]. The arterial phase helps detect arterial injuries, specifically pseudoaneurysms and arteriovenous fistulas, while the venous phase helps to differentiate contained vascular injuries from active bleeding [66]. In our institution, arterial and dual-energy portal venous phases are performed as a routine protocol. In addition, DECT delayed phase is performed only in indicated cases.

With IOIs of DECT, the active extravasation is conspicuous and can be easily differentiated from osseous fragments in cases of comminuted pelvic fractures or foreign bodies [67]. Diminished or loss of bowel wall enhancement is one of the specific signs of significant bowel injury [68] which can be well demonstrated on IOIs [55•, 57].

Delayed phase is required to further evaluate injuries identified on the portal venous phase [68]. Active bleeding appears as persistent contrast spillage with an attenuation value higher than that of the aorta on delayed images, while pseudoaneurysms remain focal and follow the attenuation of the aorta [69]. Delayed images are also helpful in differentiating life-threatening massive arterial bleeds from insidious low-flow venous bleeds [67]. In our experience, delayed phase DECT with IOI can improve the detection of slow flow venous bleeding that is not obvious on arterial and portal venous phases. Accumulation of iodine within the delayed images results in increased iodine density on the delayed images (Fig. 8).

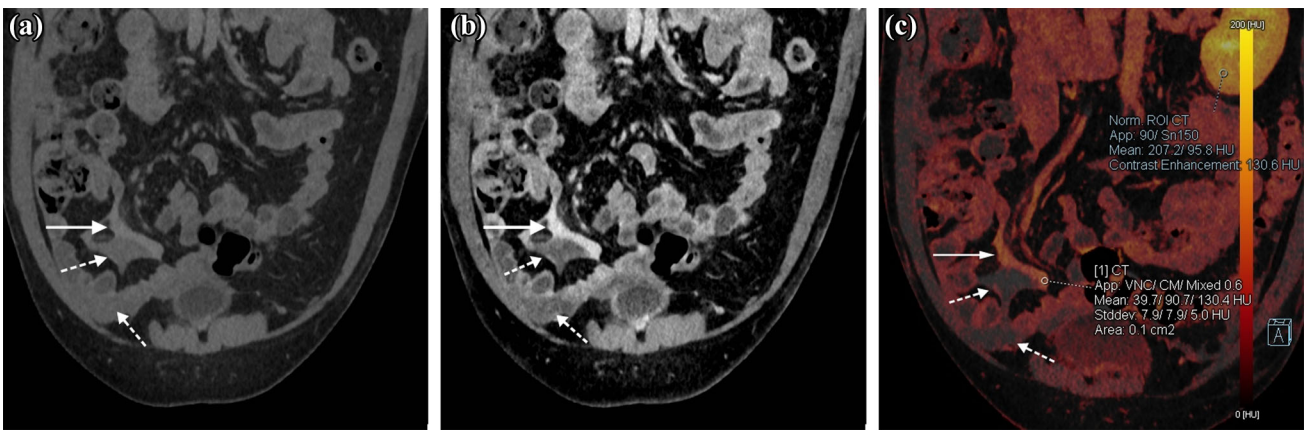

Fig. 8 A 39-year-old male after MVC, there was no active arterial bleeding on arterial phases (not shown). **a** Coronal 5 min-delayed mixed CT, **b** VMI, **c** IOI: demonstrate slowly accumulating contrast (*arrow*) adjacent to mesenteric hematoma (*dotted arrows*). VMI and IOI increase the diagnostic confidence of slowly accumulating venous bleeding which can be easily differentiated from the adjacent hematoma. A partial-thickness mesenteric laceration was repaired intraoperatively

Conclusions

The applications and scope of DECT continue to soar due to ongoing innovations, which help discriminate between different materials and tissues. To date, DECT has demonstrated a promising role in diagnosis of gastrointestinal bleeding evidenced by improving imaging quality using virtual non-contrast images and iodine overlay images, respectively. In evaluation of bowel malignancy, DECT has the potential to facilitate the detection and local staging of colon cancer as well as the characterization of metastatic regional lymph nodes. DECT can accentuate the hypoperfusion and hyperenhancement of the bowel wall relative to normally enhancing bowel, which has been shown to increase the diagnostic accuracy of inflammatory bowel conditions and bowel ischemia, respectively. Severity of traumatic bowel and mesenteric injuries can be assessed with high accuracy utilizing low-energy spectrum virtual monoenergetic reconstructions and iodine overlay imaging.

Definition Attenuation Ratio of a material: X-ray attenuation coefficients at low versus high kVp (peak kilovoltage).

Compliance with Ethical Standards

Conflict of interest Ismail Tawakol Ali, Cyrus Thomas, Khaled Y. Elbanna, Mohammed F. Mohammed, and Ferco H. Berger each declare no potential conflicts of interest. Faisal Khosa is the recipient of the Canadian Association of Radiologists/Canadian Radiological Foundation Leadership Scholarship (2017).

Human and Animal Rights and Informed Consent This article does not contain any studies with human or animal subjects performed by any of the authors.

References

Papers of particular interest, published recently, have been highlighted as:
- Of importance

1. • Marin D, Boll DT, Mileto A, Nelson RC. State of the art: dual-energy CT of the abdomen. Radiology. 2014;271(2):327–42. *This reference described the functions and foundations of dual-energy CT's applications within the abdomen. They also went into detail describing the principles on which dual energy CT operate and outlined the various sequences that can be used with this feature*.
2. Patel BN, Alexander L, Allen B, Berland L, Borhani A, Mileto A, et al. Dual-energy CT workflow: multi-institutional consensus on standardization of abdominopelvic MDCT protocols. Abdom Radiol. 2016;6:1–12.
3. Henzler T, Fink C, Schoenberg SO, Schoepf UJ. Dual-energy CT: radiation dose aspects. AJR Am J Roentgenol. 2012;199(5):16–25.
4. Rutherford RA, Pullan BR. Isherwood I Measurement of effective atomic number and electron density using an EMI scanner. Neuroradiology. 1976;11(1):15–21.
5. Kruger RA, Riederer SJ, Mistretta CA. Relative properties of tomography, K-edge imaging and K-edge tomography. Med Phys. 1977;4(3):244–9.
6. Nogueira M, Tardaguila G, Mera D, Martinez M, Tardaguila FM. Acute mesenteric ischemia: the actual role of dual-energy CT and its future potential. Eur Soc Radiol. 2016. doi:10.1594/ecr2016/C-0666.
7. Heye T, Dual-Energy CT. Applications in the Abdomen. AJR Am J Roentgenol. 2012;199:S64–70.
8. Leng S, Shiung M, Ai S, Qu M, Vrtiska TJ, Grant KL, et al. Feasibility of discriminating uric acid from non-uric acid renal stones using consecutive spatially registered low-and high-energy scans obtained on a conventional CT scanner. Am J Roentgenol. 2015;204:92–7.
9. Johnson TRC, Krauß B, Sedlmair M, Grasruck M, Bruder H, Morhard D, et al. Material differentiation by dual energy CT: initial experience. Eur Radiol. 2007;17(6):1510–7.
10. Primak AN, Ramirez Giraldo JC, Liu X, Yu L, McCollough CH. Improved dual-energy material discrimination for dual-source CT by means of additional spectral filtration. Med Phys. 2009;36(4):1359–69.
11. Silva AC, Morse BG, Hara AK, Paden RG, Hongo N, Pavlicek W. Dual-energy (spectral) CT: applications in abdominal imaging. RadioGraphics. 2011;31(4):1031–46.
12. Wu L, Xu J, Yin Y, Qu X. Usefulness of CT angiography in diagnosing acute gastrointestinal bleeding: A meta-analysis. World J Gastroenterol. 2010;16(31):3957–63.
13. Grasruck M, Kappler S, Reinwand M, Stierstorfer K. Dual energy with dual source CT and kVp switching with single source CT: a comparison of dual energy performance. Proc SPIE. 2009;7258(72):583R.
14. Wu EH, Kim SY, Wang ZJ, Chang WC, Zhao LQ, Yeh BM. Appearance and frequency of gas interface artifacts involving small bowel on rapid-voltage-switching dual-energy CT iodine-density images. Am J Roentgenol. 2016;206(2):301–6.
15. Fornaro J, Leschka S, Hibbeln D, Butler A, Anderson N, Pache G, et al. Dual- and multi-energy CT: approach to functional imaging. Insights Imaging. 2011;2(2):149–59.
16. Hartman R, Kawashima A, Takahashi N, Silva A, Vrtiska T, Leng S, et al. Applications of dual-energy ct in urologic imaging: an update. Radiol Clin North Am. 2012;50(2):191–205.
17. Yu L, Christner J, Leng S, Wang J, Fletcher JG, McCollough CH. Virtual monochromatic imaging in dual-source dual-energy CT: radiation dose and image quality. Med Phys. 2011;38(12):6371.
18. Yu L, Leng S, McCollough CH. Dual-energy CT-based monochromatic imaging. AJR Am J Roentgenol. 2012;199(5):9–15.
19. Holmes DR, Fletcher JG, Apel A, Huprich JE. Evaluation of non-linear blending in dual-energy computed tomography. NIH Public Access. 2009;68(3):409–13.
20. Ascenti G, Krauss B, Mazziotti S, Mileto A, Settineri N, Vinci S, et al. Dual-energy computed tomography (DECT) in renal masses. Nonlinear versus linear blending. Acad Radiol. 2012;19(10):1186–93.
21. Ascenti G, Mileto A, Krauss B, Gaeta M, Blandino A, Scribano E, et al. Distinguishing enhancing from nonenhancing renal masses with dual-source dual-energy CT: iodine quantification versus standard enhancement measurements. Eur Radiol. 2013;23(8):2288–95.
22. Lourenco P, Rawski R, Mohammed M, Darras K, Nicolaou S, McLaughlin P. Dual-energy computed tomography and iodine mapping are superior to conventional CT in the diagnosis of early and established intestinal ischemia and infarction. Radiological Society of North America 2015 Scientific Assembly and Annual Meeting, November 29–December 4, 2015, Chicago IL. www.archive.rsna.org/2015/15016800.html. Accessed 20 April 2017.

23. Lourenco P, Rawski R, McLaughlin P, O'Connell T, Nicolaou S. Dual-energy CT and virtual monoenergetic reconstructions: utility of novel and basic algorithms in assessment of intestinal wall enhancement and applications for acute intestinal Ischemia. Radiological Society of North America 2015 Scientific Assembly and Annual Meeting, November 29–December 4, 2015, Chicago IL. www.archive.rsna.org/2015/15016859.html. Accessed 20 April 2017.
24. Qu M, Ehman E, Fletcher JG, Huprich JE, Hara AK, Silva AC, et al. Toward biphasic computed tomography (CT) enteric contrast: material classification of luminal bismuth and mural iodine in a small-bowel phantom using dual-energy CT. J Comput Assist Tomogr. 2012;36(5):554–9.
25. Mongan J, Rathnayake S, Fu Y, Gao D-W, Yeh BM. Extravasated contrast material in penetrating abdominopelvic trauma: dual-contrast dual-energy CT for improved diagnosis–preliminary results in an animal model. Radiology. 2013;268(3):738–42.
26. Rathnayake S, Mongan J, Torres AS, Colborn R, Gao DW, Yeh BM, et al. In vivo comparison of tantalum, tungsten, and bismuth enteric contrast agents to complement intravenous iodine for double-contrast dual-energy CT of the bowel. Contrast Media Mol Imaging. 2016;11(4):254–61.
27. Kilcoyne A, Kaplan JL, Gee MS. Inflammatory bowel disease imaging: current practice and future directions. World J Gastroenterol. 2016;22(3):917–32.
28. • Fulwadhva UP, Wortman JR, Sodickson AD. Use of dual-energy CT and iodine maps in evaluation of bowel disease. radiographics. 2016;36:393–406. *This reference has a detailed description of the current utilities od DECT in assessment of bowel disease as well as its limitations and future diagnostic potential*.
29. ElSayes K, Al-Hawar M, Jagdish J, Ganesh H, Platt J. CT Enterography: principles, trends, and interpretation of findings. Radiographics. 2010;30:1955–71.
30. Apfaltrer P, Meyer M, Meier C, Henzler T, Barraza JM, Dinter DJ, et al. Contrast-enhanced dual-energy CT of gastrointestinal stromal tumors: is iodine-related attenuation a potential indicator of tumor response? Invest Radiol. 2012;47(1):65–70.
31. Rao P, Rhea J, Novelline R, Mostafavi A, McCabe C. Effect of computed tomography of the appendix on treatment of patients and use of hospital resources. Cancer Chemother Pharmacol. 1998;338:141–6.
32. Pinto Leite N, Pereira JM, Cunha R, Pinto P, Sirlin C. CT evaluation of appendicitis and its complications: imaging techniques and key diagnostic findings. Am J Roentgenol. 2005;185(2):406–17.
33. Singh A, Gervais D, Hanh P, Sagar P, Meuller P, Novelline R. Appendagitis and its mimics 1 objectives. RadioGraphics. 2005;1605(6):1521–34.
34. Neugut AI, Jacobson JS, Suh S, Mukherjee R, Arber N. The epidemiology of cancer of the small bowel. Cancer Epidemiol Prev Biomark. 1998;7(3):243–51.
35. Ganeshan D, Bhosale P, Yang T, Kundra V. Imaging features of carcinoid tumors of the gastrointestinal tract. AJR Am J Roentgenol. 2013;201(4):773–86.
36. • Shinya T, Inai R, Tanaka T, Akagi N, Sato S, Yoshino T, et al. Small bowel neoplasms: enhancement patterns and differentiation using post-contrast multiphasic multidetector CT. Abdom Radiol. 2016; 1–8. *This reference described the use of dual energy CT to identify enhancement patterns associated with small bowel neoplasia. The usefulness in this paper is in their differentiation between the types of small bowel neoplasia—such as stromal and neuroendocrine tumors–and how they present with dual energy scanning*.
37. Martin SS, Pfeifer S, Wichmann JL, Albrecht MH, Leithner D, Lenga L, et al. Noise-optimized virtual monoenergetic dual-energy computed tomography: optimization of kiloelectron volt settings in patients with gastrointestinal stromal tumors. Abdom Radiol. 2016;42(3):718–26.
38. Diculescu M, Jacob R, Croitoru A, Becheanu G, Popeneciu V. The important of histopathological and clinical variables in predicting the evolution of colon cancer. Rom J Gastroenterol. 2002;11(3):183–9.
39. Gong HX, Zhang KB, Wu LM, Baigorri BF, Yin Y, Geng X, et al. Dual energy spectral CT imaging for colorectal cancer grading: a preliminary study. PLoS ONE. 2016;11(2):1–10.
40. Neri E, Turini F, Cerri F, Faggioni L, Vagli P, Naldini G, et al. Comparison of CT colonography versus conventional colonoscopy in mapping the segmental location of colon cancer before surgery. Abdom Imaging. 2010;35(5):589–95.
41. McArthur DR, Mehrzad H, Patel R, Dadds J, Pallan A, Karandikar SS, et al. CT colonography for synchronous colorectal lesions in patients with colorectal cancer: initial experience. Eur Radiol. 2010;20(3):621–9.
42. Schaeffer B, Johnson TRC, Mang T, Kreis ME, Reiser MF, Graser A. Dual-energy CT colonography for preoperative "one-stop" staging in patients with colonic neoplasia. Acad Radiol. 2014;21(12):1567–72.
43. Gollub MJ, Schwartz LH, Akhurst T. Update on colorectal cancer imaging. Radiol Clin N Am. 2007;45(1):85–118.
44. Chen CY, Hsu JS, Jaw TS, Wu DC, Shih MCP, Lee CH, et al. Utility of the iodine overlay technique and virtual nonenhanced images for the preoperative T staging of colorectal cancer by dual-energy CT with tin filter technology. PLoS ONE. 2014;9(12):1–16.
45. Kato T, Uehara K, Ishigaki S, Nihashi T, Arimoto A, Nakamura H, et al. Clinical significance of dual-energy CT-derived iodine quantification in the diagnosis of metastatic LN in colorectal cancer. Eur J Surg Oncol. 2015;41(11):1464–70.
46. Sun H, Hou XY, Xue HD, Li XG, Jin ZY, Qian JM, et al. Dual-source dual-energy CT angiography with virtual non-enhanced images and iodine map for active gastrointestinal bleeding: image quality, radiation dose and diagnostic performance. Eur J Radiol. 2015;84(5):884–91.
47. Geffroy Y, Rodallec M, Boulay-Coletta I. Multidetector CT angiography in acute gastrointestinal bleeding: why, when, and how. Radiographics. 2011;31:35–46.
48. Graça BM, Freire PA, Brito JB, Ilharco JM, Carvalheiro VM, Caseiro-Alves F. Gastroenterologic and radiologic approach to obscure gastrointestinal bleeding: how, why, and when? Radiographics. 2010;30(1):235–52.
49. Yeh BM, Shepherd JA, Wang ZJ, Seong Teh H, Hartman RP, Prevrhal S. Dual-energy and low-kVp CT in the abdomen. Am J Roentgenol. 2009;193(1):47–54.
50. Coursey CA, Nelson RC, Boll DT, Paulson EK, Ho LM, Neville AM, et al. Dual-energy multidetector CT: how does it work, what can it tell us, and when can we use it in abdominopelvic imaging? Radiographics. 2010;30(4):1037–55.
51. Artigas JM, Martí M, Soto JA, Esteban H, Pinilla I, Guillén E. Multidetector CT angiography for acute gastrointestinal bleeding: technique and findings. Radiographics. 2013;33(5):1453–70.
52. Furukawa A, Kanasaki S, Kono N, Wakamiya M, Tanaka T, Takahashi M, et al. CT diagnosis of acute mesenteric ischemia from various causes. Am J Roentgenol. 2009;192(2):408–16.
53. Ricci ZJ, Mazzariol FS, Kaul B, Oh SK, Chernyak V, Flusberg M, et al. Hollow organ abdominal ischemia, part II: clinical features, etiology, imaging findings and management ☆. J Clin Imaging. 2016;40(4):751–64.
54. Dhatt HS, Behr SC, Miracle A, Wang ZJ, Yeh BM. Radiological evaluation of bowel Ischemia. Radiol Clin North Am. 2015;53(6):1241–54.
55. • Potretzke TA, Brace CL, Lubner MG, Sampson LA, Willey BJ, Lee FT. Early small-bowel ischemia: dual-energy CT improves

conspicuity compared with conventional CT in a swine model. Radiology. 2015;275(1):119–26. *The importance of this references stems from the study's investigation of monochromatic imaging of small bowel ischemia. Their reported values suggest a two-fold difference from what is currently seen with conventional CT.*

56. • Wallace AB, Raptis CA, Mellnick VM. Imaging of bowel Ischemia. Curr Radiol Rep. 2016;4(6):29. *The importance of this reference is due to their subjective analysis of iodine overlays to discriminate between ischemic and perfused segments within the small bowel.*
57. Darras KE, Mclaughlin PD, Kang H, Black B, Walshe T, Chang SD, et al. Virtual monoenergetic reconstruction of contrast-enhanced dual energy CT at 70 keV maximizes mural enhancement in acute small bowel obstruction. Eur J Radiol. 2016;85(5):950–6.
58. Macari M, Babb J. Hemorrhage: CT evaluation. 2003:177–84.
59. Tijssen MPM, Hofman PAM, Stadler AAR, Van Zwam W, De Graaf R, Van Oostenbrugge RJ, et al. The role of dual energy CT in differentiating between brain haemorrhage and contrast medium after mechanical revascularisation in acute ischaemic stroke. Eur Radiol. 2014;24(4):834–40.
60. Phan CM, Yoo AJ, Hirsch JA, Nogueira RG, Gupta R. Differentiation of Hemorrhage from iodinated contrast in different intracranial compartments using dual-energy head CT. Am J Neuroradiol. 2012;33:1088–94.
61. Smith JE, Midwinter M, Lambert AW. Avoiding cavity surgery in penetrating torso trauma: the role of the computed tomography scan. Ann R Coll Surg Engl. 2010;92(6):486–8.
62. Shanmuganathan K, Mirvis SE, Chiu WC, Killeen KL, Hogan GJ, Scalea TM. Penetrating torso trauma: triple-contrast helical CT in peritoneal violation and organ injury–a prospective study in 200 patients. Radiology. 2004;231(3):775–84.
63. Mongan J, Rathnayake S, Fu Y, Gao D-W, Yeh BM. Extravasated contrast material in penetrating abdominopelvic trauma: dual-contrast dual-energy CT for improved diagnosis–preliminary results in an animal model. Radiology. 2013;268(3):738–42.
64. Brofman N, Atri M, Hanson J, Grinblat L, Chughtai T, Brenneman F. Evaluation of bowel and mesenteric blunt trauma with multidetector CT. Eur Rev Med Pharmacol Sci. 2015;19(9):1589–94.
65. Scaglione M, Iaselli F, Sica G, Feragalli B, Nicola R. Errors in imaging of traumatic injuries. Abdom Imaging. 2015;40(7):2091–8.
66. Iacobellis F, Ierardi AM, Mazzei MA, Biasina AM, Carrafiello G, Nicola R, et al. Dual-phase CT for the assessment of acute vascular injuries in high-energy blunt trauma: the imaging findings and management implications. Br J Radiol. 2016;89:201.
67. Uyeda JW, Patino M, Sahani DV. Dual-energy CT in the acute abdomen. Curr Radiol Rep. 2015. doi:10.1007/s40134-015-0099-7.
68. Soto JA, Anderson SW. Multidetector CT of blunt abdominal trauma. Radiologys. 2012;265(3):678–93.
69. Stuhlfaut JW, Anderson SW, Soto JA. Blunt abdominal trauma: current imaging techniques and CT Findings in patients with Solid organ, bowel, and mesenteric injury. Semin Ultrasound, CT MRI. 2007;28(2):115–29.